2796 *Biochemistry* **2010,** *49,* 2796–2804
DOI: 10.1021/bi901388t

BIOCHEMISTRY
including biophysical chemistry & molecular biology
*Article*

# Characterization of an Atypical γ-Secretase Complex from Hematopoietic Origin†

Lisa Placanica,‡,§ Jennifer W. Chien,‡,§ and Yue-Ming Li*,‡,§

‡*Molecular Pharmacology and Chemistry Program, Memorial Sloan Kettering Cancer Center, New York, New York 10065, and* §*Department of Pharmacology, Joan Weill Graduate School of Medical Science of Cornell University, New York, New York 10021*

*Received August 10, 2009; Revised Manuscript Received February 22, 2010*

ABSTRACT: γ-Secretase is a widely expressed multisubunit enzyme complex which is involved in the pathogenesis of Alzheimer disease and hematopoietic malignancies through its aberrant processing of the amyloid precursor protein (APP) and Notch1, respectively. While γ-secretase has been extensively studied, there is a dearth of information surrounding the activity, composition, and function of γ-secretase expressed in distinct cellular populations. Here we show that endogenous γ-secretase complexes of hematopoietic origin are distinct from epithelial derived γ-secretase complexes. Hematopoietic γ-secretase has reduced activity for APP and Notch1 processing compared to epithelial γ-secretase. Characterization of the active complexes with small molecule affinity probes reveals that hematopoietic γ-secretase has an atypical subunit composition with significantly altered subunit stoichiometry. Furthermore, we demonstrate that these discrete complexes exhibit cell-line specific substrate selectivity suggesting a possible mechanism of substrate regulation. These data underscore the need for studying endogenous γ-secretase to fully understand of the biology of γ-secretase and its complexity as a molecular target for the development of disease therapeutics.

γ-Secretase processes a wide range of substrates including the amyloid precursor protein (APP),[1] Notch, ErbB4, nectin 1α, N-cadherin, and other type I transmembrane proteins, reflecting the multitude of physiological functions of this protease (*1*, *2*). Cleavage of APP by γ-secretase releases β-amyloid (Aβ) 40 and 42 peptides. Oligomerization of these peptides, specifically Aβ42, is thought to play a causative role in the pathogenesis of Alzheimer's disease (AD) (*3*, *4*). Notch1 is another well-studied substrate of γ-secretase, and it is known to play a pivotal role in lymphocyte development (*5*). Aberrant Notch1 signaling contributes to T cell acute lymphoblastic leukemia and is associated with a variety of cancers (*6*−*10*). γ-Secretase activity is associated with a multisubunit transmembrane complex comprised of at least four known subunits: presenilin (PS), nicastrin (Nct), anterior pharynx defective (Aph), and presenilin enhancer 2 (Pen2) (*11*, *12*). PS is thought to contain the catalytic core of the enzyme as it has previously been shown that active site-directed inhibitors specifically label PS, and mutation of either of the two transmembrane aspartates results in loss of γ-secretase activity (*13*−*16*). Aph and Nct have been shown to contribute to complex stability and substrate recognition, respectively, while Pen2 is necessary for the final maturation of γ-secretase (*17*−*22*). PS exists as two homologues, PS1 and PS2, which have redundant but nonoverlapping functions and are found in mutually exclusive complexes (*23*, *24*). Additionally, Aph exists as three isoforms which have also been shown to be part of mutually exclusive complexes: Aph1aL, Aph1aS, and Aph1b (*25*, *26*). Recent data have suggested that there are six possible γ-secretase complexes consisting of Nct and Pen2 with either PS1 or PS2 and one of the three Aph isoforms (2 PS × 3 Aph) with a 1:1:1:1 stoichiometry (*27*, *28*). Recent data have also revealed that TMP21 and CD147 may be putative γ-secretase subunits, but their contribution to enzyme activity and their role in the regulation of γ-secretase have not been fully elucidated (*29*−*31*).

Previous studies examining the activity and regulation of γ-secretase have utilized the exogenous expression of one or more of the components or substrates of γ-secretase in a limited number of cellular models. However, it is known that exogenous overexpression of PS1 can lead to the total replacement of endogenous PS1 along with the accumulation of full-length PS, which is not observed under endogenous conditions (*32*). Furthermore, we have previously demonstrated that γ-secretase complexes exist in a dynamic equilibrium and exogenous expression of individual subunits can cause perturbations to this equilibrium, resulting in alteration of enzyme activity (*33*). Therefore, in order to elucidate the physiological function and regulation of γ-secretase, it is critical to characterize endogenous γ-secretase complexes isolated from different cellular sources and tissue systems.

In the present study we have used a small molecule approach to characterize γ-secretase complexes from diverse cellular origins. We reveal that endogenous γ-secretase derived from hematopoietic origins is distinct from classically studied epithelial derived γ-secretase. Hematopoietic-derived γ-secretase displays an atypical subunit composition with an altered PS1-NTF:PS1-CTF ratio and a unique activity profile compared to epithelial γ-secretase.

## EXPERIMENTAL PROCEDURES

*Cell Lines*. Snap-frozen log phase growth cell culture pellets of suspension-adapted HeLa, suspension-adapted 293T, Bjab, Jurkat, and HL60 were obtained from the National Cell Culture

†This work is supported by NIH Grant R01-AG026660 (Y.-M.L.) and the Alzheimer Association (Y.-M.L.). L.P. and J.W.C. were supported by Institutional Training Grant T32 GM073546.

*To whom correspondence should be addressed at the Molecular Pharmacology and Chemistry Program, Memorial Sloan Kettering Cancer Center. Tel: 646-888-2193. Fax: 646-422-0640. E-mail: liy2@mskcc.org.

[1]Abbreviations: AD, Alzheimer disease; Aph, anterior pharynx defective; APP, amyloid precursor protein; CTF, C-terminal fragment; NCT, nicastrin; NTF, N-terminal fragment; Pen2, presenilin enhancer 2; PS, presenilin; WBC, white blood cells.

 Published on Web 02/23/2010 

Center. Mono- and polymorphonuclear white blood cells (WBC) were isolated and pooled from 1 L of porcine whole blood (Pel-Freez) using Polymorphprep (Axis-Shield) as per the manufacturer's instructions. Following isolation, WBCs were washed twice with phosphate-buffered saline and frozen at −80 °C until membrane preparation.

*Chemical Compounds and Antibodies*. L685,458 (L458), compound E, GSI34, and compound **5** was prepared and characterized as previously described (*16*, *34*, *35*). Antibodies against PS1-NTF, recognizing the 1−25 amino acid residues of PS1, were a kind gift of Dr. Min-tain Lai (Merck Research Laboratories). Antibodies against PS2-CTF (PC235) and PS1-CTF (MAB5232 and AB5308) were purchased from Calbiochem and Chemicon, respectively. Antibodies against Nct and NICD1 (SM320) were generated in our laboratory. Antibody against Pen2 (ab18189) was purchased from Abcam.

*Membrane Preparation and in Vitro γ-Secretase Assay*. Total membrane was isolated from the indicated cell lines as described (*33*, *36*). Briefly, cell pellets were resuspended in buffer A (50 mM MES, pH 6.0, 150 mM KCl, 5 mM $CaCl_2$, 5 mM $MgCl_2$, and protease inhibitors) and lysed by passage through a French press. After removal of nuclear debris by low-speed centrifugation, the total membrane fraction was isolated by pelleting at 100000*g* for 1 h. A portion of total membranes was solubilized with 1% CHAPSO in buffer A for 1 h at 4 °C, and nonsolubilized material was removed by ultracentrifugation at 100000*g* for 1 h. Protein concentration was determined with the DC protein assay kit (Bio-Rad) as per the manufacturer's instructions. *In vitro* γ-secretase activity was measured as described previously using ECL technology (*36*, *37*). Total membrane or CHAPSO-solubilized membrane was incubated in buffer B (50 mM PIPES, pH 7.0, 150 mM KCl, 5 mM $CaCl_2$, 5 mM $MgCl_2$, and protease inhibitors) with 0.25% CHAPSO, biotinylated APP, or Notch1 substrate for 2.5 h at 37 °C (APP substrate) or 2 h at 37 °C (Notch1 substrate). The reaction mix was incubated with ruthenylated G2-10 (Aβ40), ruthenylated G2-11 (Aβ42), or SM320 (NICD1) in conjunction with ruthenylated anti-rabbit in buffer C (1× PBS with 0.5% (v/v) Tween-20) for 2 h at 25 °C, and streptavidin magnetic beads (Dynel) were added. Aβ40, Aβ42, and NICD1 production was measured by ECL on an ECL reader and expressed as relative light units (RLU).

*Affinity Capture of Endogenous γ-Secretase and Western Blotting*. CHAPSO-solubilized membranes were captured as described previously (*33*). The captured complexes were eluted with 2× Laemmli sample buffer and separated by SDS−PAGE. The following antibodies were used for Western blotting: PS1-NTF 1:1000, PS1-CTF 1:1000, Nct 1:1000, and PS2-CTF 1:1000. Anti-mouse or anti-rabbit HRP-conjugated (Amersham) secondary antibodies were used in conjunction with standard ECL detection methods. PS1-NTF and PS1-CTF detection was done on a single blot without stripping; the blot was first probed with rabbit PS1-NTF, extensively washed with PBS−Tween, and then reprobed with mouse PS1-CTF. In all cases, blots shown are representative of three or more experiments.

*Photolabeling of γ-Secretase*. Total membrane or CHAPSO-solubilized membrane was photolabeled as previously described (*14*). Briefly, membrane samples were incubated in the presence or absence of 2 μM L458 in buffer B for 0.5 h at 37 °C. Compound **5** (20 nM) was added for an additional 1 h at 37 °C, and the samples were cross-linked at 350 nm on ice for 0.75 h. Following cross-linking, the reaction was denatured with RIPA buffer (50 mM Tris, pH 8.0, 150 mM NaCl, 0.1% (w/v) SDS, 1% (v/v) NP-40, and 0.5% (w/v) deoxycholic acid) for 1 h at 25 °C. Streptavidin−agarose was added and allowed to incubate overnight at 4 °C. The labeled complexes were washed with RIPA buffer and eluted with 2× Laemmli sample buffer. Samples were Western blotted as described above. In all cases, blots shown are representative of three or more experiments.

## RESULTS

*Hematopoietic Cell Lines Have Reduced γ-Secretase Activity for both APP and Notch1 Processing Compared to Epithelial Cell Lines*. To begin to characterize endogenous γ-secretase complexes, we determined γ-secretase activity levels in a panel of human cell lines derived from epithelial (HeLa and HEK293T) or hematopoietic (Bjab, Jurkat, and HL60) origins. *In vitro* γ-secretase activity was determined using total membrane or CHAPSO-solubilized membrane fractions and recombinant APP or Notch1 substrates. The epithelial cell lines, HeLa and 293T, exhibited the highest specific γ-secretase activity for processing of APP. The rate of Aβ40 and Aβ42 production for HeLa and HEK293 cell membrane was 2−5-fold higher than the hematopoietic cell lines, Bjab, Jurkat, and HL60 (Figure 1a, right and middle panels, $p < 0.01$). Since the Aβ40 and Aβ42 products were assayed using different antibodies, we compared their relative rates. The relative rate for Aβ40 and Aβ42 production was very similar for both total membrane and solubilized membrane γ-secretase activity, indicating that all cell lines exhibited a similar preference for the Aβ40 over the Aβ42 cleavage site of APP (Figure 1a, right panel). Similar to APP γ-secretase activity, HeLa and 293T had the highest levels of Notch1 γ-secretase activity than Bjab, Jurkat, and HL60 (Figure 1b). The hematopoietic cell lines had between 5- and 50-fold less Notch1 γ-secretase activity (Figure 1b, $p < 0.01$). To compare relative rate, we calculated the relative Aβ40:NICD1 rate ratio from total membrane for the various cell lines. HeLa, 293T, and Bjab all had a similar Aβ40:NICD1 ratio of approximately 30, indicating that their γ-secretase complexes have similar substrate selectivity for APP compared to Notch1. Jurkat and HL60 had a Aβ40:NICD1 ratio of 81 and 184, respectively, indicating that γ-secretase complexes in these cell lines have altered substrate selectivity and strongly favor APP as a substrate compared to HeLa, 293T, and Bjab (Figure 1c).

*Hematopoietic Cell Lines Have Significantly Reduced Levels of PS1-CTF Relative to PS1-NTF and Possess an Atypical Active γ-Secretase Complex*. The combined *in vitro* γ-secretase activity data suggest that epithelial and hematopoietic cell lines possess distinct complexes which exhibit differing levels of activity and substrate selectivity. We examined the protein levels of Nct, PS1-NTF/CTF, and PS2-CTF by Western blotting to determine if a reduction in the core catalytic and substrate binding subunits could account for the altered levels of relative activity. An equal amount of either total membrane or solubilized membrane was separated by SDS−PAGE and Western blotted for the indicated proteins. HeLa and 293T cell lines had slightly more Nct, PS1-NTF, and Pen2 compared to the hematopoietic cell lines Bjab, Jurkat, and HL60 for both total membrane and solubilized membrane fractions (Figure 2a, upper two panels and bottom panel, respectively). Strikingly, Bjab, Jurkat, and HL60 had significantly less PS1-CTF compared to HeLa and 293T for both total membrane and solubilized membrane fractions (Figure 2a, third panel). We confirmed this phenomenon using

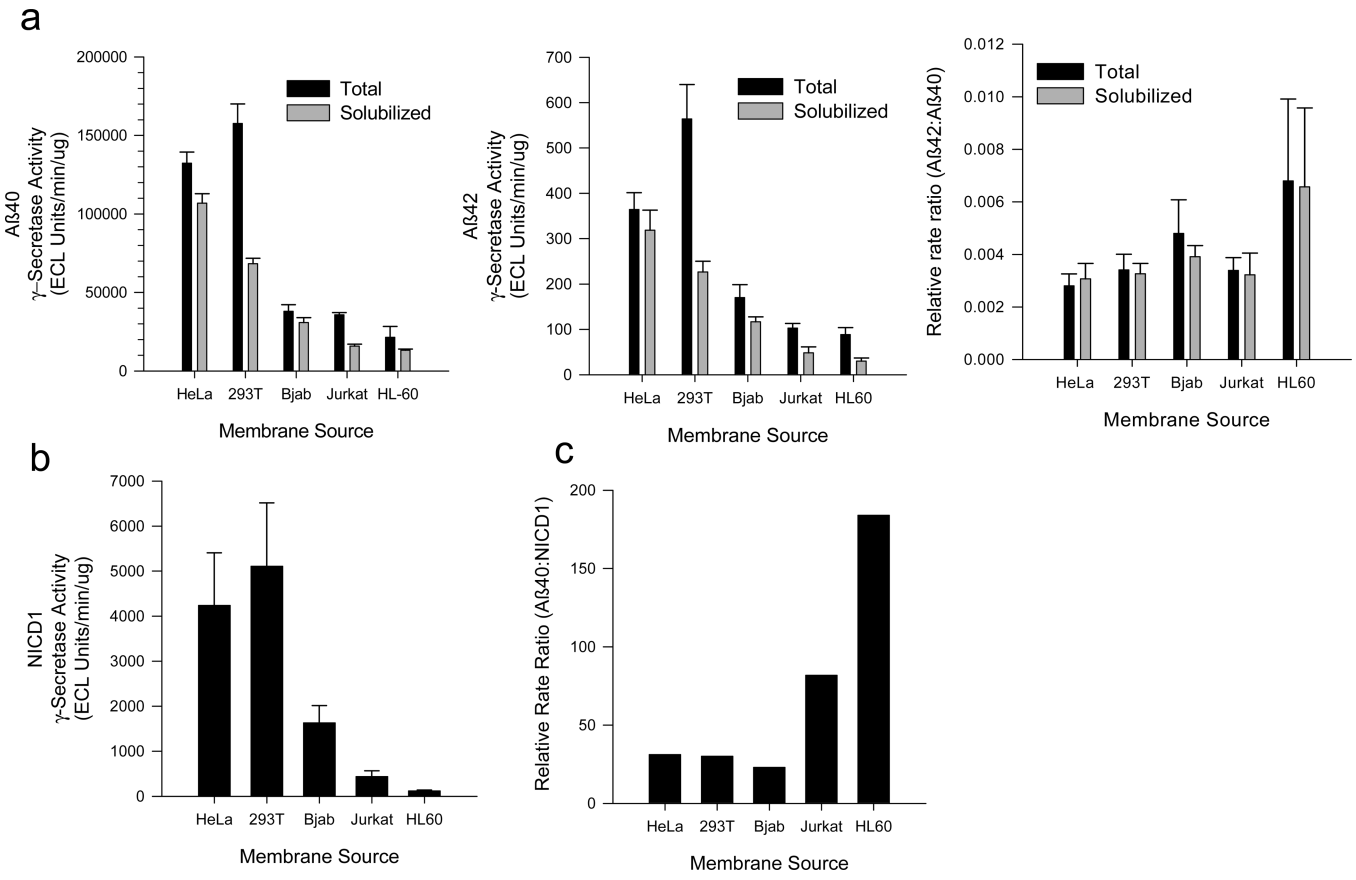


FIGURE 1: $\gamma$-Secretase isolated from cells of hematopoietic origin has reduced activity compared to epithelial-derived $\gamma$-secretase. (a) Total membrane (4 $\mu$g) (black bars) or CHAPSO-solubilized membrane (gray bars) from epithelial (HeLa and 293T) or hematopoietic (Bjab, Jurkat, HL60) origin was assayed for $\gamma$-secretase activity using a recombinant APP substrate. Background was defined as the activity remaining in the presence of 1 $\mu$M L458. Values are the average of background-subtracted activity and are represented as units $min^{-1}\,\mu g^{-1}$ (average, $n = 6 \pm$ SEM) for A$\beta$40 production (left panel) or A$\beta$42 production (middle panel). A$\beta$42:A$\beta$40 ratios (right panel) were calculated from the data presented in the left and middle panel (average, $n = 6 \pm$ SEM). (b) Total membrane (4 $\mu$g) from epithelial (HeLa and 293T) or hematopoietic (Bjab, Jurkat, HL60) origin was assayed for $\gamma$-secretase activity using a recombinant Notch1 substrate. Background was defined as the activity remaining in the presence of 1 $\mu$M L458. Values are the average of background-subtracted activity and are represented as units $min^{-1}\,\mu g^{-1}$ (average, $n = 6 \pm$ SEM). (c) The relative A$\beta$40:NICD1 ratio was calculated from the data presented in panel a (left panel) and panel b.

two other PS1-CTF antibodies with different epitopes (data not shown). To ensure that the difference in PS1-NTF/CTF level between the cell lines was not do to an artifact created during membrane preparation or solubilization, we measured the expression of PS1-NTF and PS1-CTF in whole cell lysates of the five cell lines (Figure 2b). Like the Western blot data from membrane and solubilized membrane, the hematopoietic cell lines had reduced levels of PS1-CTF compared to the epithelial cell lines but roughly equal amounts of PS1-NTF. Therefore, the hematopoietic cell lines displayed a distinct PS1-NTF:CTF ratio compared to the epithelial cell lines. PS2-CTF expression did not correlate with cell line lineage as Nct and PS1-NTF/CTF expression did. The 293T cells had the highest expression of PS2-CTF, HeLa and Bjab had slightly less PS2-CTF than 293T, and Jurkat and HL60 had undetectable levels of PS2-CTF (Figure 2a, fourth panel).

In order to ensure that the observed increase in the relative PS1-NTF:CTF ratio of the hematopoietic cell lines was truly reflective of a cell lineage specific characteristic, we quantitated the amount of PS1-NTF and PS1-CTF in HeLa and Bjab CHAPSO-solubilized membrane. Increasing amounts of protein (1.25−5 $\mu$g) of HeLa (Figure 2c, left panel) or Bjab (Figure 2c, right panel) were resolved by SDS−PAGE and Western blotted for PS1-CTF and PS1-NTF to determine the dynamic range of detection. The relative band intensity was determined by measuring the area under the curve (AUC) using ImageJ quantification software, and the linear range of detection for both PS1-NTF and PS1-CTF for HeLa (left panel) and Bjab (right panel) was determined to be between 2.5 and 5 $\mu$g of solubilized membrane (Figure 2c). We therefore resolved 3 $\mu$g of solubilized membrane in quadruplicate by SDS−PAGE and determined the relative AUC for PS1-NTF and PS1-CTF for HeLa and Bjab (Figure 2d). Solubilized membrane from HeLa had approximately 4-fold more PS1-NTF than from Bjab but approximately 15-fold more PS1-CTF. These data confirmed that Bjab exhibited a significantly different PS1-NTF:CTF ratio compared to HeLa ($p < 0.001$).

Because only a small percentage of expressed PS is engaged in active $\gamma$-secretase complexes, Western blotting alone does not distinguish between active and inactive $\gamma$-secretase complexes (*23*, *33*, *38*). Therefore, it is possible that the increased relative PS1-NTF:CTF ratio observed for the hematopoietic cell lines does not reflect the actual ratio in the active complex. We recently developed a second generation active site affinity probe, compound **5** (Figure 3a), which has been used to examine mouse brain endogenous active $\gamma$-secretase complexes (*35*). We measured the ability of compound **5** to inhibit *in vitro* $\gamma$-secretase activity in solubilized membrane fractions using a recombinant APP substrate; compound **5** had equal potency in all five cell lines. Compound **5** was incubated with the solubilized membrane

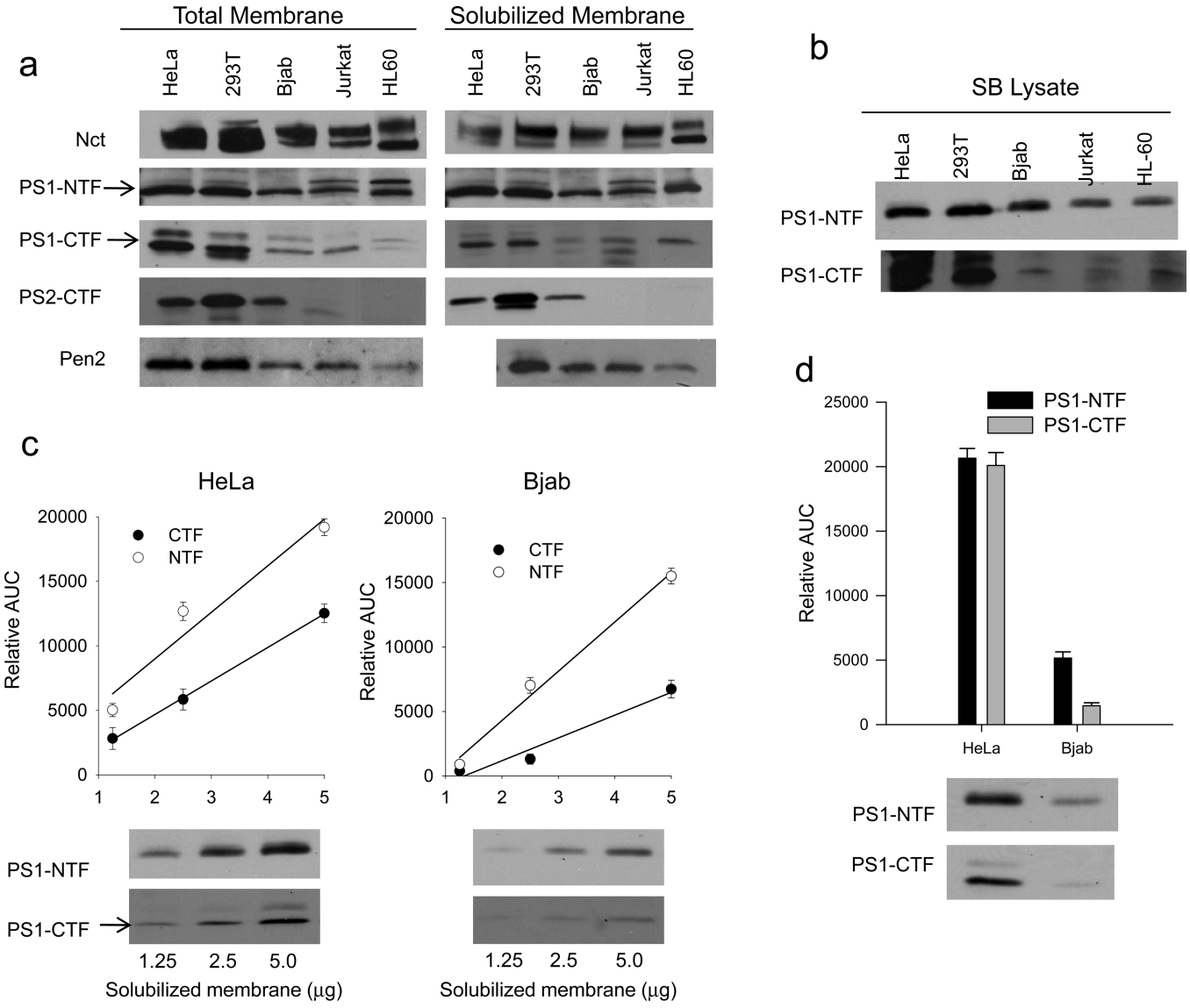


FIGURE 2: Hematopoietic $\gamma$-secretase complexes have reduced levels of PS1-CTF compared to epithelial $\gamma$-secretase. (a) 10 $\mu$g total membrane (left panel) or CHAPSO-solubilized membrane (right panel) was separated by SDS−PAGE and Western blotted for the indicated components of $\gamma$-secretase. (b) Cells ($1 \times 10^6$) were directly lysed by boiling in 100 $\mu$L of Laemmli sample buffer. The lysate (20 $\mu$L) was separated by SDS−PAGE and Western blotted for the indicated components of $\gamma$-secretase. (c) The dynamic range for detection of PS1-NTF and PS1-CTF was determined to be between 2.5 and 5 $\mu$g. Increasing micrograms of HeLa or Bjab CHAPSO-solubilized membrane was separated by SDS−PAGE and Western blotted for PS1-NTF and PS1-CTF. The relative area under the curve (AUC) was determined by measuring the band intensities using ImageJ quantification software. (d) Bjab has a 4-fold higher relative PS1-NTF:CTF ratio compared to HeLa. CHAPSO-solubilized membrane (3 $\mu$g) was separated by SDS−PAGE in quadruplicate and Western blotted for PS1-NTF and PS1-CTF (representative lanes shown, lower left panel). The relative AUC (upper left panel) was determined by measuring the band intensities using ImageJ quantification software (average, $n = 4 \pm$ SEM).

fraction in the presence or absence of L458, and the bound complexes were isolated with strepavidin−agarose under native conditions, resolved by SDS−PAGE, and Western blotted for the indicated proteins. In all cases, capture by compound **5** was blocked by inclusion of excess L458, indicating that the capture was specific (Figure 3b). Similar amounts of both Nct and PS1-NTF were captured with compound **5** from all five cell lines (Figure 3b, top two panels). On the contrary, significantly less PS1-CTF was captured by compound **5** from Bjab, Jurkat, and HL60 in comparison to HeLa and 293T (Figure 3b). Overall, this caused a 2−20-fold difference in the relative PS1-NTF:CTF ratio for the hematopoietic cell lines compared to the epithelial cell lines. These data parallel the Western blotting data and confirm that active hematopoietic $\gamma$-secretase complexes contain a distinctive PS1-NTF:PS1-CTF ratio compared with the epithelial protease.

In order to confirm that this difference truly refected the ratio of PS1-NTF and PS1-CTF within the active $\gamma$-secretase complex in cell membranes, we analyzed photolabeled species using compound **5**. Compound **5** also contains a photoreactive benzophenone group which can be used to covalently label the active site of $\gamma$-secretase (Figure 3a, gray highlight), which has the same core structure of L852,505 (*14*). Our recent studies indicated that L852,505 also labels PS1-NTF when the labeled proteins were detected with anti-PS1 antibody against the 1−25 amino acid residues of PS1 (*39*), which was not recognizable using an antibody against the 1−14 amino acid residues of PS1 (*14*). Compound **5** was incubated with either solubilized membrane or total membrane in the presence or absence of excess L458. After irradiation, photolabeled proteins were solubilized, captured, eluted, and analyzed by Western analysis. Compound **5** was able to label roughly equal amounts of PS1-NTF from both

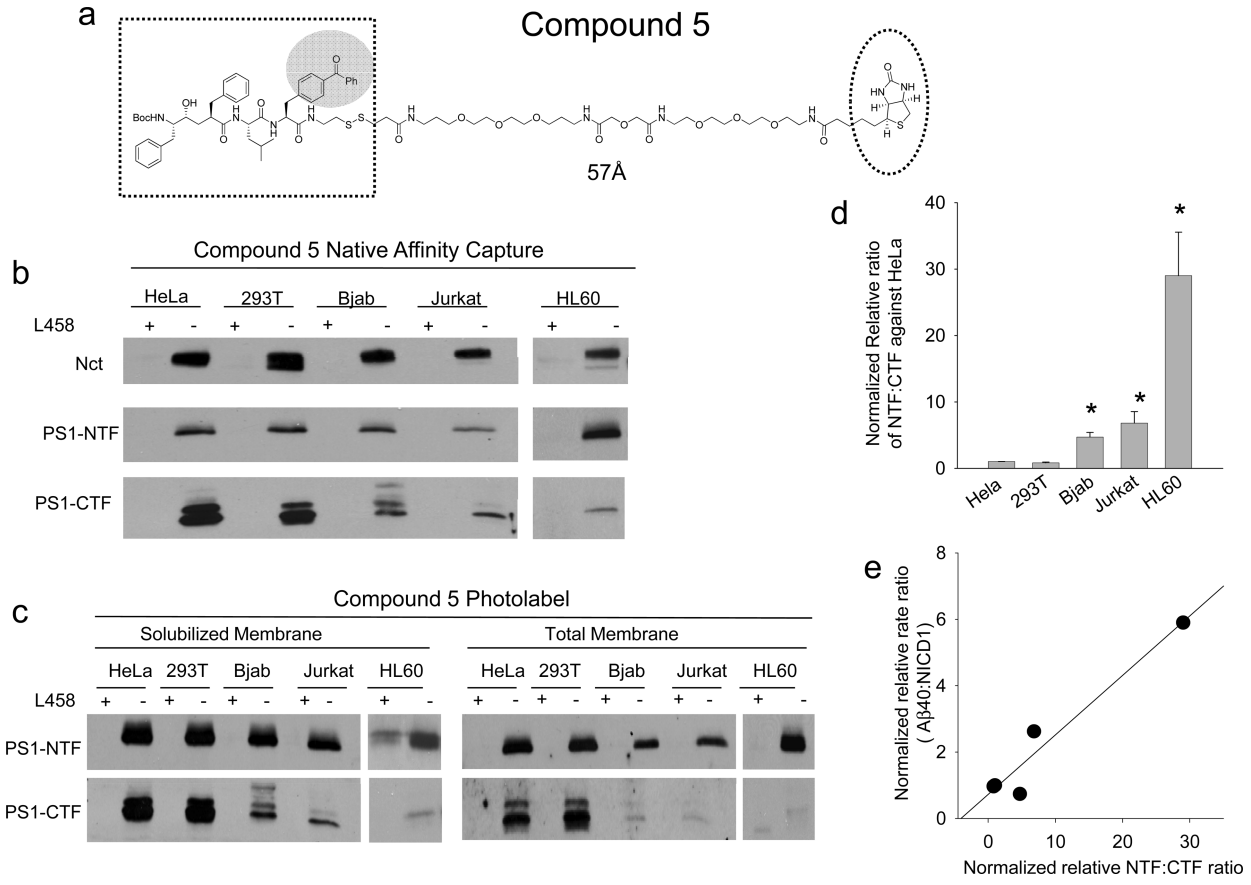


FIGURE 3: Hematopoietic $\gamma$-secretase has reduced incorporation of PS1-CTF into active complexes compared to epithelial $\gamma$-secretase. (a) Chemical structure of compound **5**. The parental L458 backbone is delineated by the dashed box and the biotin moiety by the dashed oval, and the photoreactive benzophenone group is highlighted with a shaded gray circle. The linear distance of the linker between the parental backbone and the biotin moiety is measured in angstroms (Å) as determined with 3D ChemDraw. (b) Active hematopoietic $\gamma$-secretase complexes contain reduced amounts of PS1-CTF relative to PS1-NTF. Active $\gamma$-secretase complexes in the native conformation were isolated from 800 $\mu$g of CHAPSO-solubilized membrane protein with 20 nM compound **5** in the presence (+) or absence (−) of 2 $\mu$M L458. The isolated complexes were resolved by SDS−PAGE and Western blotted for the indicated components of $\gamma$-secretase. The HL-60 sample was analyzed from a separated gel which included Hela membrane as an internal control. (c) The active site of the hematopoietic $\gamma$-secretase complex exhibits reduced photolabeling of PS1-CTF compared to epithelial $\gamma$-secretase. CHAPSO-solubilized (left panel) or total membrane (right panel) was photolabeled with 20 nM compound **5** in the presence (+) or absence (−) of 2 $\mu$M L458. Following denaturation with RIPA buffer, the labeled proteins were isolated with streptavidin−agarose, resolved by SDS−PAGE, and Western blotted for PS1-NTF or PS1-CTF as indicated. (d) Normalized relative ratios of PS1-NTF:PS1-CTF. The relative area under the curve (AUC) was calculated by measuring the band intensities of PS1-NTF and PS1-CTF from panel b and panel c using ImageJ quantification software. Each relative ratio was normalized or divided by the ratio of HeLa from the same set of blots. The ratio represented the average of ratios in panel b and panel c ($p < 0.01$). (e) The relationship between the normalized ratios of NTF:CTF and A$\beta$40:NICD1.

solubilized and total membrane fractions of all five cell lines (Figure 3c). Labeling was completely blocked by inclusion of excess nonbiotinylated L458, indicating that the labeling was specific (Figure 3c). Much less PS1-CTF was photolabeled in Bjab, Jurkat, and HL60 compared to HeLa and 293T (Figure 3c, bottom panel) for both solubilized membrane and, even more strikingly, total membrane. In order to reduce the variation between different Western blot analyses, we determined the relative ratio of PS1-NTF:PS1-CTF in each cell line and then normalized them against HeLa membrane (i.e., the normalized ratio for HeLa membranes equals 1). This conversion allows direct comparison of blots from separate studies. Consequently, we averaged normalized ratios from Figure 3b,c and found the ratio in Bjab, Jurkat, and HL60 is significantly higher than in HeLa and 293T (Figure 3d). These analyses rule out that the differences between these cells resulted from variations of CHAPSO solubilization and support our finding that hematopoietic cell lines contain an atypical $\gamma$-secretase complex which has an altered relative PS1-NTF:CTF ratio. Moreover, we found that a positive correlation ($R = 0.97$) exists between normalized NTF:CTF ratio and A$\beta$40:NICD1 ratio (Figure 3e).

To further confirm whether an atypical $\gamma$-secretase exists in hematopoietic cells, we carried out the same study using white blood cells (WBC) isolated from whole porcine blood. Mononuclear and polymorphonuclear leucocytes were separated from anticoagulated porcine blood and pooled, and the total membrane fraction was isolated. Porcine WBC $\gamma$-secretase exhibited a rate of 3674 A$\beta$40 units min$^{-1}$ $\mu$g$^{-1}$ and 1225 NICD1 units min$^{-1}$ $\mu$g$^{-1}$ of total membrane. Porcine WBC A$\beta$40 activity could be inhibited by L458 in a dose-dependent manner (Figure 4a). Western blotting revealed that WBC had less Nct and PS1-NTF when compared to HeLa total membrane, consistent with the lower *in vitro* activity levels (Figure 4b, top two panels). Interestingly, porcine WBC PS1-NTF was slightly larger than HeLa PS1-NTF, likely reflecting species-specific processing of PS. Like the other hematopoietic cell lines examined, WBC had very low expression of PS1-CTF; this was confirmed with two different antibodies (Figure 5b, panels 3 and 4). Therefore, we

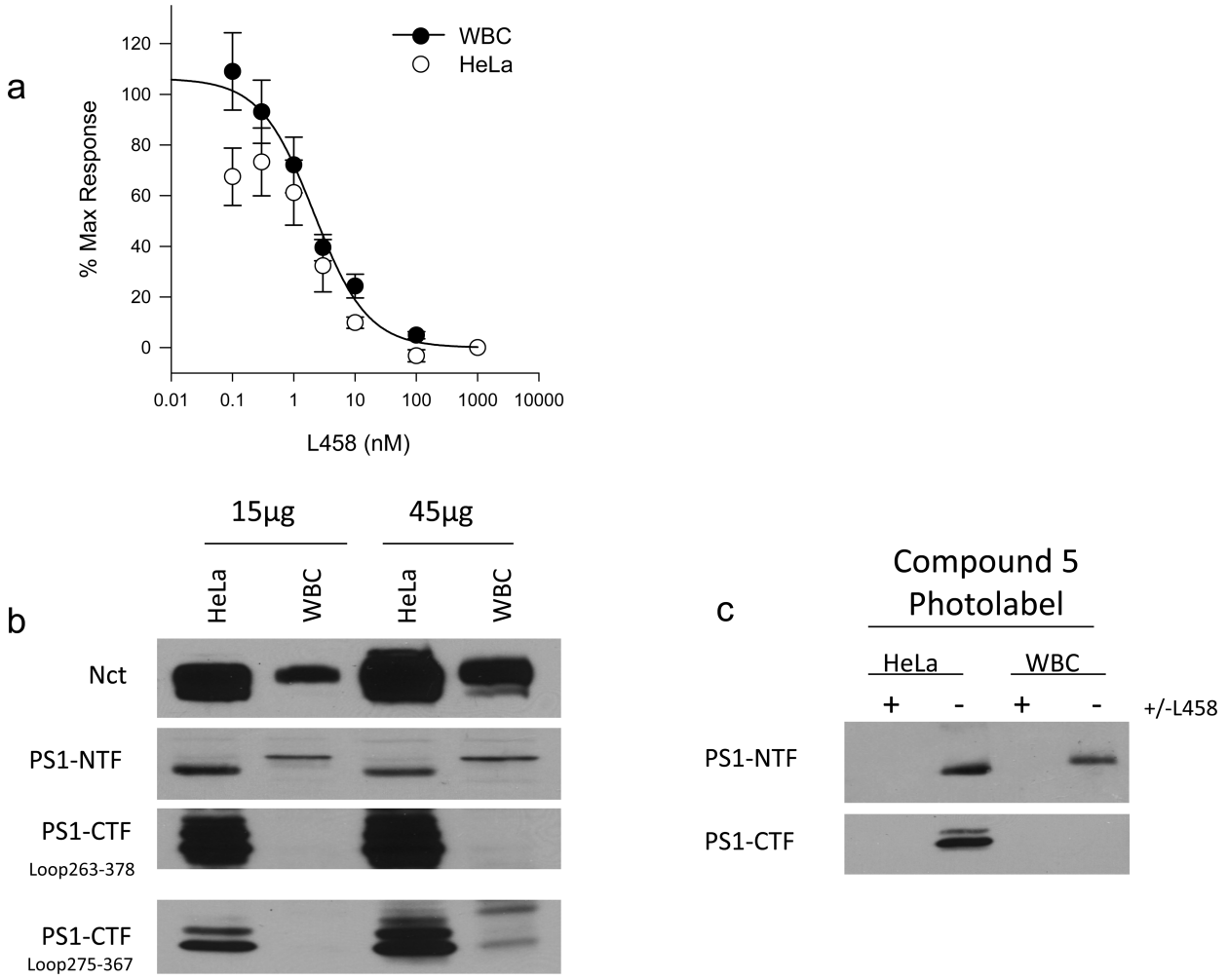


FIGURE 4: The active site of the porcine WBC $\gamma$-secretase complex exhibits reduced photolabeling of PS1-CTF compared to HeLa $\gamma$-secretase. (a) Membrane was incubated with increasing concentrations of L458 and assayed for *in vitro* A$\beta$40 activity using a recombinant APP substrate. (b) Indicated amounts of total membrane from HeLa and WBC were Western blotted for the Nct, PS1-NTF, and PS1-CTF. (c) CHAPSO total membrane was photolabeled with 20 nM compound **5** in the presence (+) or absence (−) of 2 $\mu$M L458. Following denaturation with RIPA buffer, the labeled proteins were isolated with streptavidin−agarose, resolved by SDS−PAGE, and Western blotted for PS1-NTF or PS1-CTF as indicated.

conclude that porcine WBC, like the human hematopoietic cell lines, has much less PS1-CTF relative to PS1-NTF.

To confirm that the Western blotting data reflect the composition of active $\gamma$-secretase complexes, we used compound **5** to covalently photolabel PS1-NTF and PS1-CTF from total membrane. While compound **5** was clearly able to photolabel WBC PS1-NTF, labeling of WBC PS1-CTF was undetectable whereas equal amounts of HeLa PS1-NTF and PS1-CTF were labeled (Figure 4c). These results are identical to the compound **5** photolabeling of total membrane from Bjab, Jurkat, and HL60 (Figure 4, right panel) and further confirm that cells of hematopoietic origin have an atypical active $\gamma$-secretase complex which exhibits a greatly increased relative PS1-NTF:CTF ratio.

*Hematopoietic $\gamma$-Secretase Cannot Be Pharmacological Distinguished from Classically Epithelial $\gamma$-Secretase*. We have clearly established that cells of hematopoietic origin contain distinct $\gamma$-secretase complexes compared to the classically studied epithelial-derived $\gamma$-secretase; hematopoietic $\gamma$-secretase has lower overall activity, differing relative substrate selectivity, and an atypical subunit composition. We wanted to determine if hematopoietic $\gamma$-secretase had a unique pharmacological profile which could be used to distinguish it from epithelial $\gamma$-secretase. *In vitro* APP $\gamma$-secretase activity in solubilized membrane was measured in the presence of increasing concentrations of three structurally diverse small molecule $\gamma$-secretase inhibitors: a peptidomimetic (L458), a sulfonamide (GSI34), and a benzodiazepine (compound E). There was no difference between the cell lines in the potency of the small molecule inhibitors screened, indicating that these small molecules cannot distinguish between the two classes of $\gamma$-secretase (Figure 5).

## DISCUSSION

The existence of discrete $\gamma$-secretase complexes has long been inferred from biochemical and expression data (*25*, *40*−*42*). However, the findings described here are the first which demonstrate the existence of unique complexes using purely endogenous sources. We have clearly shown that hematopoietic $\gamma$-secretase is distinct from the classically studied epithelial $\gamma$-secretase in both activity and subunit composition; hematopoietic $\gamma$-secretase has lower *in vitro* activity, displays unique substrate selectivity, and has an atypical PS1-NTF:CTF stoichiometry incorporated into active complexes compared to epithelial $\gamma$-secretase.

Previous studies have suggested that the core $\gamma$-secretase subunits are arrayed with a 1:1:1:1:1 stoichiometry (*27*, *28*, *43*).

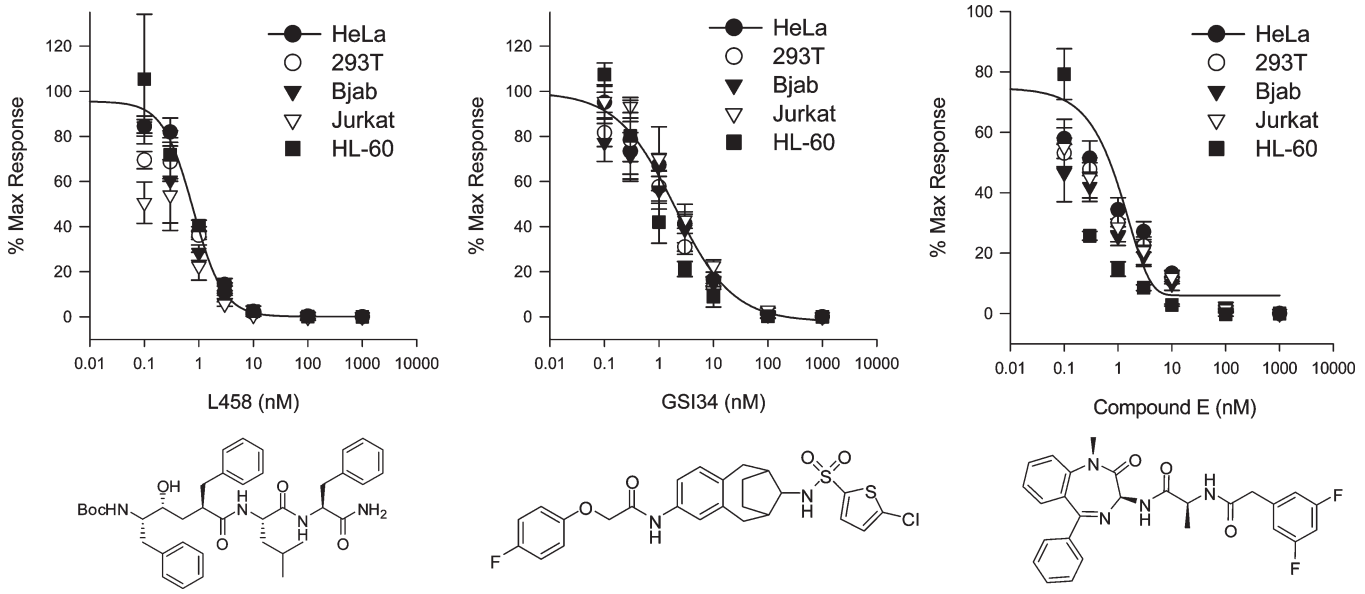


FIGURE 5: Small molecule inhibitors cannot distinguish between epithelial and hematopoetic $\gamma$-secretase activity. 4 $\mu$g of CHAPSO-solubilized membrane was incubated with increasing concentrations of distinct classes of $\gamma$-secretase inhibitor and assayed for *in vitro* A$\beta$40 activity using a recombinant APP substrate. Compound structures shown below $IC_{50}$ curves were generated in SigmaPlot 8.0 (average, $n = 4 \pm$ SEM).

Our laboratory has previously shown that the complex stoichiometry is dynamic and can be altered by exogenous expression of $\gamma$-secretase subunits or PS FAD mutants (*33*). Our work here further supports this dynamic nature of the $\gamma$-secretase complex stoichiometric arrangement and, importantly, does so using purely endogenous cell models. While we cannot conclude the precise amount of each subunit present, it is clear that the relative ratio of PS1-NTF to PS1-CTF is clearly different between hematopoietic and epithelial $\gamma$-secretase. The finding that the relative PS1-NTF:CTF ratio is greatly altered in hematopoietic $\gamma$-secretase is surprising as $\gamma$-secretase is a diaspartyl protease with both catalytic aspartates required for activity (*13*). The $\gamma$-secretase complex is formed in a tightly regulated stepwise fashion, and subunit stability is dependent on complex formation: an initial subcomplex is formed between Nct and Aph, followed by the incorporation of full-length holo-PS, and finally incorporation of Pen2 (*11*, *17*, *44*−*46*). The incorporation of Pen2 promotes the endoproteolysis of holo-PS into its stably associated PS-NTF and PS-CTF fragments; this endoproteolysis converts an inactive complex into a catalytically competent enzyme, partitions the catalytic aspartates into separate fragments, and is required for $\gamma$-secretase activity (*12*, *47*−*50*). It is likely that catalytic activity of any $\gamma$-secretase complex is driven by a 1:1 array of PS1-NTF:PS1-CTF which maintains the catalytic diaspartyl stoichiometry. Therefore, the reduced catalytic activity seen in hematopoietic $\gamma$-secretase compared to epithelial $\gamma$-secretase can be accounted for by a reduction in the amount of PS1-CTF which would decrease the number of 1:1 NTF:CTF catalytic units in the active complexes. The unpaired hematopoietic PS1-NTF units may contribute the altered substrate selectivity seen for Jurkat and HL60 $\gamma$-secretase as these cell lines exhibited the most robust increase in relative PS1-NTF:CTF ratio and altered substrate selectivity in comparison to the other cell lines examined; indeed, our data demonstrated that the relative ratio of NTF:CTF does in fact correlate with the relative rate ratios of $\gamma$-seccretase for A$\beta$40 and NICD1 production (see Figure 3e). However, the precise mechanism of the NTF:CTF ratio and its correlation with substrate specificity as well as the exact physiological function of the catalytically unpaired PS1-NTF in hematopoietic $\gamma$-secretase require further investigation.

In addition, these data also indicate that the levels of PS1-NTF and CTF in hematopoietic $\gamma$-secretase appear to be independently regulated. There have been reports which have shown that it is in fact possible for PS1-CTF expression levels to vary independently of PS1-NTF levels. During zebrafish embryogenesis, PS1-CTF levels were shown to increase relative to holo-PS levels, suggesting selective regulation of PS1-CTF (*51*). Selective phosphorylation of PS1-CTF has also been shown to play a role in regulation of PS1-CTF levels. Kirschenbaum et al. previously demonstrated that PS1-CTF levels could be reduced independently of PS1-NTF levels through phosphorylation by glycogen synthase kinase-3$\beta$ (*52*). Likewise, overexpression of cyclin-dependent kinase-5/p35 has been shown to lead to the selective stabilization of phosphorylated PS1-CTF in 293T cells (*53*). Further investigation is required to clarify how such an atypical $\gamma$-secretase complex is assembled and/or regulated in cells of hematopoietic origin.

$\gamma$-Secretase is known to process a wide range of type I transmembrane proteins with limited primary sequence homology (*1*, *54*). The exact mechanism by which $\gamma$-secretase achieves substrate regulation is unknown. It is intriguing to note that the cell line specific complexes identified here exhibit unique patterns of relative substrate selectivity for the processing of APP and Notch1. These data, therefore, suggest that distinct $\gamma$-secretase complexes with preferential substrate processing abilities may be one potential mechanism of substrate regulation. The physiological substrates and function of these discrete $\gamma$-secretase complexes remain to be investigated.

In sum, this work further supports the existence of multiple and distinct endogenous $\gamma$-secretase complexes and underscores the complexity of $\gamma$-secretase as a molecular target for the development of therapeutics for the treatment of Alzheimer's disease and other disease states.

## ACKNOWLEDGMENT

We thank Dr. Min-tain Lai for PS1 NTF antibody.

## REFERENCES


1. Parks, A. L., and Curtis, D. (2007) Presenilin diversifies its portfolio. *Trends Genet. 23*, 140–150.
2. Evin, G., Sernee, M. F., and Masters, C. L. (2006) Inhibition of gamma-secretase as a therapeutic intervention for Alzheimer's disease: prospects, limitations and strategies. *CNS Drugs 20*, 351–372.
3. Hardy, J., and Allsop, D. (1991) Amyloid deposition as the central event in the aetiology of Alzheimer's disease. *Trends Pharmacol. Sci. 12*, 383–388.
4. Hardy, J. A., and Higgins, G. A. (1992) Alzheimer's disease: the amyloid cascade hypothesis. *Science 256*, 184–185.
5. Allman, D., Aster, J. C., and Pear, W. S. (2002) Notch signaling in hematopoiesis and early lymphocyte development. *Immunol. Rev. 187*, 75–86.
6. Jundt, F., Anagnostopoulos, I., Forster, R., Mathas, S., Stein, H., and Dorken, B. (2002) Activated Notch1 signaling promotes tumor cell proliferation and survival in Hodgkin and anaplastic large cell lymphoma. *Blood 99*, 3398–3403.
7. Jundt, F., Schwarzer, R., and Dorken, B. (2008) Notch signaling in leukemias and lymphomas. *Curr. Mol. Med. 8*, 51–59.
8. Bolos, V., Grego-Bessa, J., and de la Pompa, J. L. (2007) Notch signaling in development and cancer. *Endocr. Rev. 28*, 339–363.
9. Stylianou, S., Clarke, R. B., and Brennan, K. (2006) Aberrant activation of Notch signaling in human breast cancer. *Cancer Res. 66*, 1517–1525.
10. Talora, C., Sgroi, D. C., Crum, C. P., and Dotto, G. P. (2002) Specific down-modulation of Notch1 signaling in cervical cancer cells is required for sustained HPV-E6/E7 expression and late steps of malignant transformation. *Genes Dev. 16*, 2252–2263.
11. Iwatsubo, T. (2004) The gamma-secretase complex: machinery for intramembrane proteolysis. *Curr. Opin. Neurobiol. 14*, 379–383.
12. Takasugi, N., Tomita, T., Hayashi, I., Tsuruoka, M., Niimura, M., Takahashi, Y., Thinakaran, G., and Iwatsubo, T. (2003) The role of presenilin cofactors in the gamma-secretase complex. *Nature 422*, 438–441.
13. Wolfe, M. S., Xia, W., Ostaszewski, B. L., Diehl, T. S., Kimberly, W. T., and Selkoe, D. J. (1999) Two transmembrane aspartates in presenilin-1 required for presenilin endoproteolysis and gamma-secretase activity. *Nature 398*, 513–517.
14. Li, Y. M., Xu, M., Lai, M. T., Huang, Q., Castro, J. L., DiMuzio-Mower, J., Harrison, T., Lellis, C., Nadin, A., Neduvelil, J. G., Register, R. B., Sardana, M. K., Shearman, M. S., Smith, A. L., Shi, X. P., Yin, K. C., Shafer, J. A., and Gardell, S. J. (2000) Photoactivated gamma-secretase inhibitors directed to the active site covalently label presenilin 1. *Nature 405*, 689–694.
15. Esler, W. P., Kimberly, W. T., Ostaszewski, B. L., Diehl, T. S., Moore, C. L., Tsai, J. Y., Rahmati, T., Xia, W., Selkoe, D. J., and Wolfe, M. S. (2000) Transition-state analogue inhibitors of gamma-secretase bind directly to presenilin-1. *Nat. Cell Biol. 2*, 428–434.
16. Seiffert, D., Bradley, J. D., Rominger, C. M., Rominger, D. H., Yang, F., Meredith, J. E., Jr., Wang, Q., Roach, A. H., Thompson, L. A., Spitz, S. M., Higaki, J. N., Prakash, S. R., Combs, A. P., Copeland, R. A., Arneric, S. P., Hartig, P. R., Robertson, D. W., Cordell, B., Stern, A. M., Olson, R. E., and Zaczek, R. (2000) Presenilin-1 and -2 are molecular targets for gamma-secretase inhibitors. *J. Biol. Chem. 275*, 34086–34091.
17. Niimura, M., Isoo, N., Takasugi, N., Tsuruoka, M., Ui-Tei, K., Saigo, K., Morohashi, Y., Tomita, T., and Iwatsubo, T. (2005) Aph-1 contributes to the stabilization and trafficking of the gamma-secretase complex through mechanisms involving intermolecular and intramolecular interactions. *J. Biol. Chem. 280*, 12967–12975.
18. Shah, S., Lee, S. F., Tabuchi, K., Hao, Y. H., Yu, C., LaPlant, Q., Ball, H., Dann, C. E., 3rd, Sudhof, T., and Yu, G. (2005) Nicastrin functions as a gamma-secretase-substrate receptor. *Cell 122*, 435–447.
19. Zhang, Y. W., Luo, W. J., Wang, H., Lin, P., Vetrivel, K. S., Liao, F., Li, F., Wong, P. C., Farquhar, M. G., Thinakaran, G., and Xu, H. (2005) Nicastrin is critical for stability and trafficking but not association of other presenilin/gamma-secretase components. *J. Biol. Chem. 280*, 17020–17026.
20. Francis, R., McGrath, G., Zhang, J., Ruddy, D. A., Sym, M., Apfeld, J., Nicoll, M., Maxwell, M., Hai, B., Ellis, M. C., Parks, A. L., Xu, W., Li, J., Gurney, M., Myers, R. L., Himes, C. S., Hiebsch, R., Ruble, C., Nye, J. S., and Curtis, D. (2002) aph-1 and pen-2 are required for Notch pathway signaling, gamma-secretase cleavage of betaAPP, and presenilin protein accumulation. *Dev. Cell 3*, 85–97.
21. Prokop, S., Shirotani, K., Edbauer, D., Haass, C., and Steiner, H. (2004) Requirement of PEN-2 for stabilization of the presenilin N-/C-terminal fragment heterodimer within the gamma-secretase complex. *J. Biol. Chem. 279*, 23255–23261.
22. Watanabe, N., Tomita, T., Sato, C., Kitamura, T., Morohashi, Y., and Iwatsubo, T. (2005) Pen-2 is incorporated into the gamma-secretase complex through binding to transmembrane domain 4 of presenilin 1. *J. Biol. Chem. 280*, 41967–41975.
23. Lai, M. T., Chen, E., Crouthamel, M. C., DiMuzio-Mower, J., Xu, M., Huang, Q., Price, E., Register, R. B., Shi, X. P., Donoviel, D. B., Bernstein, A., Hazuda, D., Gardell, S. J., and Li, Y. M. (2003) Presenilin-1 and presenilin-2 exhibit distinct yet overlapping {gamma}-secretase activities. *J. Biol. Chem. 278*, 22475–22481.
24. Herreman, A., Hartmann, D., Annaert, W., Saftig, P., Craessaerts, K., Serneels, L., Umans, L., Schrijvers, V., Checler, F., Vanderstichele, H., Baekelandt, V., Dressel, R., Cupers, P., Huylebroeck, D., Zwijsen, A., Van Leuven, F., and De Strooper, B. (1999) Presenilin 2 deficiency causes a mild pulmonary phenotype and no changes in amyloid precursor protein processing but enhances the embryonic lethal phenotype of presenilin 1 deficiency. *Proc. Natl. Acad. Sci. U.S.A. 96*, 11872–11877.
25. Hebert, S. S., Serneels, L., Dejaegere, T., Horre, K., Dabrowski, M., Baert, V., Annaert, W., Hartmann, D., and De Strooper, B. (2004) Coordinated and widespread expression of gamma-secretase in vivo: evidence for size and molecular heterogeneity. *Neurobiol. Dis. 17*, 260–272.
26. Ma, G., Li, T., Price, D. L., and Wong, P. C. (2005) APH-1a is the principal mammalian APH-1 isoform present in gamma-secretase complexes during embryonic development. *J. Neurosci. 25*, 192–198.
27. Sato, T., Diehl, T. S., Narayanan, S., Funamoto, S., Ihara, Y., De Strooper, B., Steiner, H., Haass, C., and Wolfe, M. S. (2007) Active gamma-secretase complexes contain only one of each component. *J. Biol. Chem. 282*, 33985–33993.
28. Shirotani, K., Edbauer, D., Prokop, S., Haass, C., and Steiner, H. (2004) Identification of distinct gamma-secretase complexes with different APH-1 variants. *J. Biol. Chem. 279*, 41340–41345.
29. Zhou, S., Zhou, H., Walian, P. J., and Jap, B. K. (2005) CD147 is a regulatory subunit of the gamma-secretase complex in Alzheimer's disease amyloid beta-peptide production. *Proc. Natl. Acad. Sci. U.S.A. 102*, 7499–7504.
30. Chen, F., Hasegawa, H., Schmitt-Ulms, G., Kawarai, T., Bohm, C., Katayama, T., Gu, Y., Sanjo, N., Glista, M., Rogaeva, E., Wakutani, Y., Pardossi-Piquard, R., Ruan, X., Tandon, A., Checler, F., Marambaud, P., Hansen, K., Westaway, D., George-Hyslop, P., St, and Fraser, P. (2006) TMP21 is a presenilin complex component that modulates gamma-secretase but not epsilon-secretase activity. *Nature 440*, 1208–1212.
31. Vetrivel, K. S., Gong, P., Bowen, J. W., Cheng, H., Chen, Y., Carter, M., Nguyen, P. D., Placanica, L., Wieland, F. T., Li, Y. M., Kounnas, M. Z., and Thinakaran, G. (2007) Dual roles of the transmembrane protein p23/TMP21 in the modulation of amyloid precursor protein metabolism. *Mol. Neurodegener. 2*, 4.
32. Thinakaran, G., Harris, C. L., Ratovitski, T., Davenport, F., Slunt, H. H., Price, D. L., Borchelt, D. R., and Sisodia, S. S. (1997) Evidence that levels of presenilins (PS1 and PS2) are coordinately regulated by competition for limiting cellular factors. *J. Biol. Chem. 272*, 28415–28422.
33. Placanica, L., Tarassishin, L., Yang, G., Peethumnongsin, E., Kim, S. H., Zheng, H., Sisodia, S., and Li, Y. M. (2009) PEN2 and presenilin-1 modulate the dynamic equilibrium of presenilin-1 and presenilin-2 gamma-secretase complexes. *J. Biol. Chem. 284*, 2967–2977.
34. Shearman, M. S., Beher, D., Clarke, E. E., Lewis, H. D., Harrison, T., Hunt, P., Nadin, A., Smith, A. L., Stevenson, G., and Castro, J. L. (2000) L-685,458, an aspartyl protease transition state mimic, is a potent inhibitor of amyloid beta-protein precursor gamma-secretase activity. *Biochemistry 39*, 8698–8704.
35. Placanica, L., Zhu, L., and Li, Y.-M. (2009) Gender and age dependent $\gamma$-secretase activity in mouse brain and its implication in sporadic alzheimer disease. *Plos ONE 4*, e5088.
36. Li, Y. M., Lai, M. T., Xu, M., Huang, Q., DiMuzio-Mower, J., Sardana, M. K., Shi, X. P., Yin, K. C., Shafer, J. A., and Gardell, S. J. (2000) Presenilin 1 is linked with gamma-secretase activity in the detergent solubilized state. *Proc. Natl. Acad. Sci. U.S.A. 97*, 6138–6143.
37. Yin, Y. I., Bassit, B., Zhu, L., Yang, X., Wang, C., and Li, Y. M. (2007) {gamma}-Secretase substrate concentration modulates the Abeta42/Abeta40 ratio: implications for alzheimer disease. *J. Biol. Chem. 282*, 23639–23644.
38. Beher, D., Fricker, M., Nadin, A., Clarke, E. E., Wrigley, J. D., Li, Y. M., Culvenor, J. G., Masters, C. L., Harrison, T., and Shearman, M. S. (2003) In vitro characterization of the presenilin-dependent gamma-secretase complex using a novel affinity ligand. *Biochemistry 42*, 8133–8142.

39. Shelton, C. C., Zhu, L., Chau, D., Yang, L., Wang, R., Djaballah, H., Zheng, H., and Li, Y. M. (2009) Modulation of {gamma}-secretase specificity using small molecule allosteric inhibitors. *Proc. Natl. Acad. Sci. U.S.A. 106*, 20228−20233.
40. Loewer, A., Soba, P., Beyreuther, K., Paro, R., and Merdes, G. (2004) Cell-type-specific processing of the amyloid precursor protein by presenilin during *Drosophila* development. *EMBO Rep. 5*, 405–411.
41. Oh, Y. S., and Turner, R. J. (2006) Protease digestion indicates that endogenous presenilin 1 is present in at least two physical forms. *Biochem. Biophys. Res. Commun. 346*, 330–334.
42. Gu, Y., Sanjo, N., Chen, F., Hasegawa, H., Petit, A., Ruan, X., Li, W., Shier, C., Kawarai, T., Schmitt-Ulms, G., Westaway, D., St. George-Hyslop, P., and Fraser, P. E. (2004) The presenilin proteins are components of multiple membrane-bound complexes that have different biological activities. *J. Biol. Chem. 279*, 31329–31336.
43. Shirotani, K., Tomioka, M., Kremmer, E., Haass, C., and Steiner, H. (2007) Pathological activity of familial Alzheimer's disease-associated mutant presenilin can be executed by six different gamma-secretase complexes. *Neurobiol. Dis. 27*, 102–107.
44. LaVoie, M. J., Fraering, P. C., Ostaszewski, B. L., Ye, W., Kimberly, W. T., Wolfe, M. S., and Selkoe, D. J. (2003) Assembly of the gamma-secretase complex involves early formation of an intermediate subcomplex of Aph-1 and nicastrin. *J. Biol. Chem. 278*, 37213–37222.
45. Iwatsubo, T. (2004) Assembly and activation of the gamma-secretase complex: roles of presenilin cofactors. *Mol. Psychiatry 9*, 8–10.
46. Brunkan, A. L., and Goate, A. M. (2005) Presenilin function and gamma-secretase activity. *J. Neurochem. 93*, 769–792.
47. Kim, S. H., Ikeuchi, T., Yu, C., and Sisodia, S. S. (2003) Regulated hyperaccumulation of presenilin-1 and the "gamma-secretase" complex: evidence for differential intramembranous processing of transmembrane substrates. *J. Biol. Chem. 278*, 33992−34002.
48. Hasegawa, H., Sanjo, N., Chen, F., Gu, Y. J., Shier, C., Petit, A., Kawarai, T., Katayama, T., Schmidt, S. D., Mathews, P. M., Schmitt-Ulms, G., Fraser, P. E., and St. George-Hyslop, P. (2004) Both the sequence and length of the C terminus of PEN-2 are critical for intermolecular interactions and function of presenilin complexes. *J. Biol. Chem. 279*, 46455–46463.
49. Steiner, H., Winkler, E., Edbauer, D., Prokop, S., Basset, G., Yamasaki, A., Kostka, M., and Haass, C. (2002) PEN-2 is an integral component of the gamma-secretase complex required for coordinated expression of presenilin and nicastrin. *J. Biol. Chem. 277*, 39062–39065.
50. Brunkan, A. L., Martinez, M., Walker, E. S., and Goate, A. M. (2005) Presenilin endoproteolysis is an intramolecular cleavage. *Mol. Cell. Neurosci. 29*, 65–73.
51. Nornes, S., Groth, C., Camp, E., Ey, P., and Lardelli, M. (2003) Developmental control of presenilin1 expression, endoproteolysis, and interaction in zebrafish embryos. *Exp. Cell Res. 289*, 124–132.
52. Kirschenbaum, F., Hsu, S. C., Cordell, B., and McCarthy, J. V. (2001) Glycogen synthase kinase-3beta regulates presenilin 1 C-terminal fragment levels. *J. Biol. Chem. 276*, 30701–30707.
53. Lau, K. F., Howlett, D. R., Kesavapany, S., Standen, C. L., Dingwall, C., McLoughlin, D. M., and Miller, C. C. (2002) Cyclin-dependent kinase-5/p35 phosphorylates presenilin 1 to regulate carboxy-terminal fragment stability. *Mol. Cell. Neurosci. 20*, 13–20.
54. Struhl, G., and Adachi, A. (2000) Requirements for presenilin-dependent cleavage of notch and other transmembrane proteins. *Mol. Cell 6*, 625–636.